Article

Nonpolar Isosteres of Damaged DNA Bases: Effective Mimicry of Mutagenic Properties of 8-Oxopurines

Yosuke Taniguchi, and Eric T. Kool

J. Am. Chem. Soc., **2007**, 129 (28), 8836-8844• DOI: 10.1021/ja071970q • Publication Date (Web): 26 June 2007

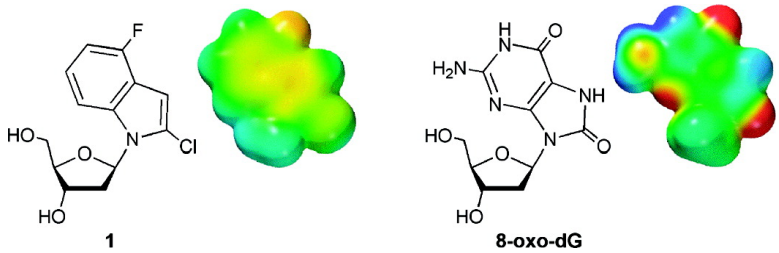

More About This Article

Additional resources and features associated with this article are available within the HTML version:

- Supporting Information
- Links to the 4 articles that cite this article, as of the time of this article download
- Access to high resolution figures
- Links to articles and content related to this article
- Copyright permission to reproduce figures and/or text from this article

View the Full Text HTML

J|A|C|S
ARTICLES
Published on Web 06/26/2007

Nonpolar Isosteres of Damaged DNA Bases: Effective Mimicry of Mutagenic Properties of 8-Oxopurines

Yosuke Taniguchi and Eric T. Kool*

Contribution from the Department of Chemistry, Stanford University, Stanford California 94305-5080

Received March 20, 2007; E-mail: kool@stanford.edu

Abstract: A substantial fraction of mutations that arise in the cell comes from oxidative damage to DNA bases. Oxidation of purine bases at the 8-position, yielding 8-oxo-G and 8-oxo-A, results in conformational changes (from anti to syn) that cause miscoding during DNA replication. Here we describe the synthesis and biophysical and biochemical properties of low-polarity shape mimics of 8-oxopurines, and we report that these new analogues exhibit remarkable mimicry of the mutagenic properties of the natural damaged bases. A 2-chloro-4-fluoroindole nucleoside (**1**) was designed as an isosteric analogue of 8-oxo-dG, and a 2-chloro-4-methylbenzimidazole nucleoside (**2**) as a mimic of 8-oxo-dA. The nucleosides were prepared by reaction of the parent heterocycles with Hoffer's chlorodeoxyribose derivative. Structural studies of the free nucleosides **1** and **2** revealed that both bases are oriented syn, thus mimicking the conformation of the oxopurine nucleosides. Suitably protected phosphoramidite derivatives were prepared for incorporation into synthetic DNAs, to be used as probes of DNA damage responses, and 5′-triphosphate derivatives (**3** and **4**) were synthesized as analogues of damaged nucleotides in the cellular nucleotide pool. Base pairing studies in 12-mer duplexes showed that **1** and **2** have low affinity for polar pairing partners, consistent with previous nonpolar DNA base analogues. However, both compounds pair with small but significant selectivity for purine partners, consistent with the idea that the syn purine geometry leads to pyrimidine-like shapes. Steady-state kinetics studies of **1** and **2** were carried out with the Klenow fragment of *Escherichia coli* DNA Pol I (exo$^-$) in single-nucleotide insertions. In the DNA template, the analogues successfully mimicked the mutagenic behavior of oxopurines, with **1** being paired selectively with adenine and **2** pairing selectively with guanine. The compounds showed similar mutagenic behavior as nucleoside triphosphate analogues, being preferentially inserted opposite mutagenic purine partners. The results suggest that much of the mutagenicity of oxopurines arises from their shapes in the syn conformation rather than from electrostatic and hydrogen-bonding effects. The new analogues are expected to be generally useful as mechanistic probes of cellular responses to DNA damage.

Introduction

One of the most important mechanisms by which mutations occur in cells is oxidative damage to DNA bases.[1] The purines in particular are susceptible to oxidation at the 8-position, and this damage can occur both to purine bases in existing DNA strands,[2] causing miscoding during DNA replication,[3] and to purine bases in the cellular nucleotide pool,[4] resulting in mispairing as they are incorporated into new DNA strands. Because of the high mutagenic potential of such oxidized bases, a number of cellular pathways have evolved to identify and repair this damage, including enzymes that recognize 8-oxo-G and 8-oxo-A in double-stranded DNA[5] and enzymes that cleave 8-oxo-dATP and 8-oxo-dGTP.[6] The topic as a whole is very actively studied because of the close connection of DNA damage and repair to the origins of cancer and its treatment.[1,7]

(1) (a) Wang, D.; Kreutzer, D. A.; Essigmann, J. M. *Mutat. Res.* **1998**, *400*, 99−115. (b) Cadet, J.; Douki, T.; Gasparutto, D.; Ravanat, J. L. *Mutat. Res.* **2003**, *531*, 5−23. (c) Barnes, D. E.; Lindahl, T. *Annu. Rev. Genet.* **2004**, *38*, 445−476. (d) Nakabeppu, Y.; Sakumi, K.; Sakamoto, K.; Tsuchimoto, D.; Tsuzuki, T.; Nakatsu, Y. *Biol. Chem.* **2006**, *387*, 373−379. (e) Wilson, D. M.; Bohr, V. A. *DNA Repair* **2007**, *6*, 544−559.

(2) (a) Dizdaroglu, M. *Biochemistry* **1985**, *24*, 4476−4481. (b) Duarte, V.; Muller, J. G.; Burrows, C. J. *Nucleic Acids Res.* **1999**, *27*, 496−502. (b) Greenberg, M. M. *Biochem. Soc. Trans.* **2004**, *32*, 46−50. (c) Hogg, M.; Wallace, S. S.; Doublie, S. *Curr. Opin. Struct. Biol.* **2005**, *15*, 86−93. (d) Russo, M. T.; De Luca, G.; Degan, P.; Bignami, M. *Mutat. Res.* **2007**, *614*, 69−76.

(3) (a) Krahn, J. M.; Beard, W. A.; Miller, H.; Grollman, A. P.; Wilson, S. H. *Structure* **2003**, *11*, 121−127. (b) Freisinger, E.; Grollman, A. P.; Miller, H.; Kisker, C. *EMBO J.* **2004**, *23*, 1494−1505.

(4) (a) Colussi, C.; Parlanti, E.; Degan, P.; Aquilina, G.; Barnes, D.; Macpherson, P.; Karran, P.; Crescenzi, M.; Dogliotti, E.; Bignami, M. *Curr. Biol.* **2002**, *12*, 912−918. (b) Macpherson, P.; Barone, F.; Maga, G.; Mazzei, F.; Karran, P.; Bignami, M. *Nucleic Acids Res.* **2005**, *33*, 5094−5105. (c) Hanes, J. W.; Thal, D. M.; Johnson, K. A. *J. Biol. Chem.* **2006**, *281*, 36241−36248.

(5) (a) Fromme, J. C.; Banerjee, A.; Verdine, G. L. *Curr. Opin. Struct. Biol.* **2004**, *14*, 43−49. (b) Bruner, S. D.; Norman, D. P.; Verdine, G. L. *Nature* **2004**, *427*, 652−656. (c) Lindahl, T. *Nature* **2004**, *427*, 598. (d) Francis, A. W.; Helquist, S. A.; Kool, E. T.; David, S. S. *J. Am. Chem. Soc.* **2003**, *125*, 16235−16242. (e) Manuel, R. C.; Hitomi, K.; Arvai, A. S.; House, P. G.; Kurtz, A. J.; Dodson, M. L.; McCullough, A. K.; Tainer, J. A.; Lloyd, R. S. *J. Biol. Chem.* **2004**, *279*, 46930−46939. (f) Pope, M. A.; David, S. S. *DNA Repair* **2005**, *4*, 91−102.

(6) (a) Saraswat, V.; Massiah, M. A.; Lopez, G.; Amzel, L. M.; Mildvan, A. S. *Biochemistry.* **2002**, *41*, 15566−15577. (b) Kamiya, H.; Yakushiji, H.; Dugue, L.; Tanimoto, M.; Pochet, S.; Nakabeppu, Y.; Harashima, H. *J. Mol. Biol.* **2004**, *336*, 843−850. (c) Nakabeppu, Y.; Kajitani, K.; Sakamoto, K.; Yamaguchi, H.; Tsuchimoto, D. *DNA Repair* **2006**, *5*, 761−772.

10.1021/ja071970q CCC: $37.00

An interesting and important aspect of 8-oxopurine structure and biochemistry is the fact that the substitution by oxygen at the 8-position can cause a flip in nucleoside conformation from anti (the standard pairing conformation in DNA) to syn.[8] Indeed, this conformation change is believed to be a chief cause of mutagenesis by oxopurines. For example, 8-oxo-G in the syn conformation is complementary to adenine in the hydrogen-bonding sense,[8,9] and 8-oxo-G often miscodes for adenine in DNA replication, both in vitro and in cells.[10,11] Similarly, 8-oxo-A also causes mispairing and mutagenesis,[12] albeit to a lesser extent. However, it is not clear whether 8-oxopurine miscoding arises from electrostatic (e.g., hydrogen bonding) effects or from the change in shape resulting from the conformational flip. In addition, there is widespread interest in how the various other enzymes that recognize and process such damage can distinguish damaged from intact bases,[5,6] and how they chemically perform their repair mechanisms. Moreover, there has been literature discussion more generally on whether syn−anti steric influences might be an important contributor to DNA replication selectivity.[13] Thus it would be useful to have molecules that could act as probes of such recognition and repair in the context of oxidative DNA damage and more generally as probes of syn−anti conformational effects.

Here we describe the synthesis and biophysical and biochemical properties of four new nonpolar nucleoside and nucleotide analogues that are designed to mimic the shapes of 8-oxopurine nucleosides. We find that these compounds effectively mimic many of the promutagenic properties of the natural oxidized nucleosides: they adopt the syn orientation, they display altered pairing preferences from this change, and they are replicated with very different pairing selectivities, just as the natural oxopurines are. Our data illustrate the large effect that changes in conformation (and thus shape) can have on pairing and replication preferences and suggest that many of the pairing and mispairing preferences of oxopurines arise primarily from their altered shapes.

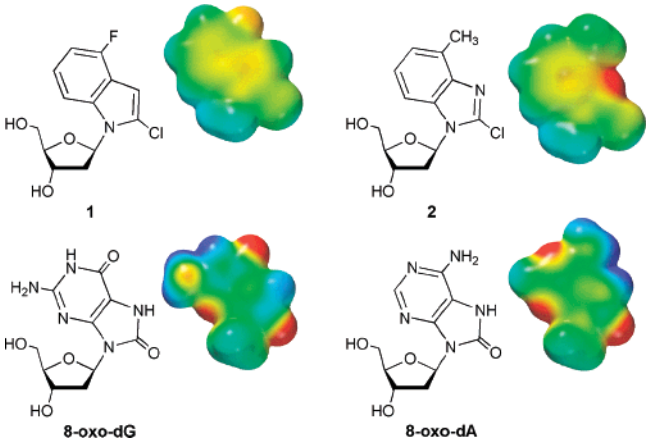

Figure 1. Structures of 8-oxopurine deoxynucleosides and of the isostere analogues **1** and **2**. Space-filling models of the bases alone are shown (methyl replacing deoxyribose), illustrating steric mimicry of the analogues for the syn edges (right-hand sides) of natural oxidatively damaged bases. Space-filling models are van der Waals surfaces with electrostatic potentials shown in color [AM1 calculations, Spartan (Wavefunction Inc.)].

Results

Design and Synthesis. Compound **1**, a previously unknown 2-chloro-4-fluoroindole nucleoside, was designed as a nonpolar isostere of *syn*-8-oxoguanine; space-filling models of this base in syn conformation show close shape mimicry of the pairing edge of oxo-G (Figure 1). The 2-chloro substituent of analogue **1** was meant to mimic the 8-oxo group and sterically drive the conformation change from anti to syn.[14] The fluoride at C-4 replaces the 6-oxo of G, while the CH group at the 3-position sterically mimics the NH at position 9 of 8-oxo-G. Although 8-oxo-G also possesses an exocyclic amino group, we omitted such a group on **1** to simplify synthesis; it is not expected to affect the pairing edge of the syn-oriented base. We prepared the 5′-dimethoxytrityl-3′-cyanoethylphosphoramidite derivative of deoxyriboside **1** for incorporation into synthetic oligonucleotides. The free nucleoside analogue **1** was also converted to the 5′-triphosphate derivative **3**; this was meant to mimic 8-oxo-dGTP and thus serve as a probe of the effects of oxidative damage in the nucleotide pool.

Compound **2** was prepared as an 8-oxo-dA analogue by 2-chlorination of a previously studied deoxyadenosine mimic (dZ) in which low-polarity 4-methylbenzimidazole replaces polar adenine.[16] Substitution of the 2-position is expected to cause a change to syn conformation, in analogy to 8-oxoadenine, which is known to prefer syn.[8] Space-filling models of the base of **2** in this conformation show a close resemblance to the size and shape of 8-oxoadenine; however, one difference is that it lacks a proton at N3, whereas 8-oxo-A has such a proton in its preferred tautomer (Figure 1). Interestingly, the base of **2** also closely resembles the size and shape of cytosine and thus could serve as a low-polarity analogue of this base with the ability to form only one canonical hydrogen bond. Finally, we prepared the 5′-triphosphate derivative of this nucleoside (compound **4**) as an analogue of the oxidatively damaged nucleotide 8-oxo-dATP.

(7) (a) Paz-Elizur, T.; Krupsky, M.; Elinger, D.; Schechtman, E.; Livneh, Z. *Cancer Biomark.* **2005**, *1*, 201−205. (b) Collins, A. R. *Eur. J. Cancer* **2005**, *41*, 1923−1930. (c) Sanchez-Perez, I. *Clin. Transl. Oncol.* **2006**, *8*, 642−646. (d) Gupta, R.; Brosh, R. M., Jr. *Curr. Med. Chem.* **2007**, *14*, 503−517.

(8) (a) Kouchakdjian, M.; Bodepudi, V.; Shibutani, S.; Eisenberg, M.; Johnson, F.; Grollman, A. P.; Patel, D. J. *Biochemistry* **1991**, *30*, 1403−1412. (b) Leonard, G. A.; Guy, A.; Brown, T.; Teoule, R.; Hunter, W. N. *Biochemistry* **1992**, *31*, 8415−8420. (c) McAuley-Hecht, K. E.; Leonard, G. A.; Gibson, N. J.; Thomson, J. B.; Watson, W. P.; Hunter, W. N.; Brown, T. *Biochemistry* **1994**, *33*, 10266−10270. (d) Lipscomb, L. A.; Peek, M. E.; Morningstar, M. L.; Verghis, S. M.; Miller, E. M.; Rich, A.; Essigmann, J. M.; Williams, L. D. *Proc. Natl. Acad. Sci. U.S.A.* **1995**, *92*, 719−723. (e) Eason, R. G.; Burkhardt, D. M.; Phillips, S. J.; Smith, D. P.; David, S. S. *Nucleic Acids Res.* **1996**, *24*, 890−897. (f) Cheng, X.; Kelso, C.; Hornak, V.; de los Santos, C.; Grollman, A. P.; Simmerling, C. *J. Am. Chem. Soc.* **2005**, *127*, 13906−13918.

(9) Ober, M.; Linne, U.; Gierlich, J.; Carell, T. *Angew. Chem., Int. Ed. Engl.* **2003**, *42*, 4947−4951.

(10) (a) Shibutani, S.; Takeshita, M.; Grollman, A. P. *Nature* **1991**, *349*, 431−434. (b) Lowe, L. G.; Guengerich, F. P. *Biochemistry* **1996**, *35*, 9840−9849. (c) Krahn, J. M.; Beard, W. A.; Miller, H.; Grollman, A. P.; Wilson, S. H. *Structure* **2003**, *11*, 121−127. (d) Hsu, G. W.; Ober, M.; Carell, T.; Beese, L. S. *Nature* **2004**, *431*, 217−221. (e) Oka, N.; Greenberg, M. M. *Nucleic Acids Res.* **2005**, *33*, 1637−1643.

(11) (a) Tan, X.; Grollman, A. P.; Shibutani, S. *Carcinogenesis* **1999**, *20*, 2287−2292. (b) Wood, M. L.; Esteve, A.; Morningstar, M. L.; Kuziemko, G. M.; Essigmann, J. M. *Nucleic Acids Res.* **1992**, *20*, 6023−6032.

(12) (a) Guschlbauer, W.; Duplaa, A. M.; Guy, A.; Teoule, R.; Fazakerley, G. V. *Nucleic Acids Res.* **1991**, *19*, 1753−1758. (b) Shibutani, S.; Bodepudi, V.; Johnson, F.; Grollman, A. P. *Biochemistry* **1993**, *32*, 4615−4621. (c) Kamiya, H.; Miura, H.; Murata-Kamiya, N.; Ishikawa, H.; Sakaguchi, T.; Inoue, H.; Sasaki, T.; Masutani, C.; Hanaoka, F.; Nishimura, S.; Ohtsuka, E. *Nucleic Acids Res.* **1995**, *23*, 2893−2899. (d) Kim, S. K.; Kim, J. Y.; Baek, A. K.; Moon, B. J. *Bioorg. Med. Chem. Lett.* **2002**, *12*, 1977−1980.

(13) (a) Sintim, H. O.; Kool, E. T. *Angew. Chem., Int. Ed.* **2006**, *45*, 1974−1979. (b) Kincaid, K. K.; Beckman, J.; Zivkovic, A.; Halcomb, R. L.; Engels, J. W.; Kuchta, R. D. *Nucleic Acids Res.* **2005**, *33*, 2620−2628. (c) Zhang, X.; Lee, I.; Berdis, A. J. *Biochemistry* **2005**, *44*, 13101−13110. (d) Adelfinskaya, O.; Nashine, V. C.; Bergstrom, D. E.; Davisson, V. J. *J. Am. Chem. Soc.* **2005**, *127*, 16000−16001.

(14) Chloro substitution was chosen over fluoro at the 2 position because of greater synthetic accessibility.

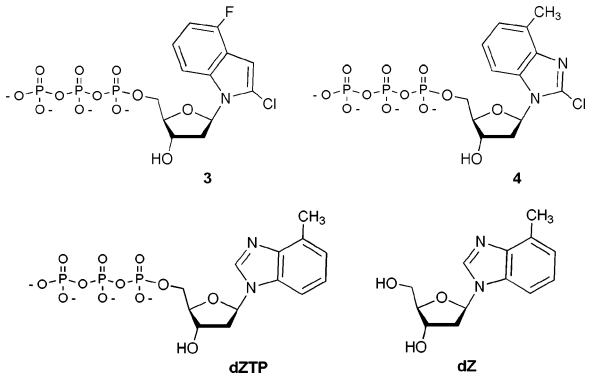

For comparison with these putatively syn nonpolar nucleosides we prepared the known nucleoside dZ, having the 4-methylbenzimidazole base. This compound has been shown to adopt an anti base conformation both as the free nucleoside and in DNA,[16] and thus it serves as a useful point of reference for **1** and **2**. In particular, dZ acts as a direct point of comparison with **2**, since it differs only in its lack of a chlorine substituent, which was designed to change the base conformation. We also prepared the nucleoside 5′-triphosphate derivative dZTP[16] for comparison with the other dNTP analogues.

Schemes 1 and 2 show the routes employed for syntheses of **1** and **2** and their phosphoramidite derivatives (**7** and **11**, respectively). The syntheses were generally straightforward; however, we noted some sensitivity of the 2-chloro group of **2** to standard ammonia DNA deprotection, and thus we employed rapid deprotection chemistry for oligonucleotides containing this compound, which allowed us to use a milder base for deprotection. In addition, mixtures of N1- and N3-isomers of toluoyl nucleoside (**9a**,**9b**) were observed in the coupling with Hoffer's chlorodeoxyribose derivative; it proved necessary to carry the ~19:1 mixture forward for one additional step before they could be chromatographically separated. Structures of the final nucleosides were confirmed by 2-D correlation and nuclear Overhauser effect spectroscopy (COSY and NOESY) experiments (see Supporting Information).

Conformation. Two-dimensional NMR structural studies of **1** and **2** in deuterated dimethyl sulfoxide (DMSO-d_6) were carried out to confirm not only the isomeric identity (above) but also the conformational preferences of the new analogues. The experiments with nucleoside **1** confirmed that this compound adopts the syn conformation in solution (see Supporting Information), consistent with a recent report of 8-haloguanine nucleosides, all of which were found to adopt the syn conformation.[15] Similar results were found for compound **2**. Previous structural studies have shown that the base of dZ adopts an anti conformation[16] (as does adenine in dA); once the chlorinated nucleoside **2** was prepared, solution structural studies confirmed the switch to syn as a result of the halogen substitution (see Supporting Information).

Base Stacking and Pairing Properties in DNA. To study the biophysical and biochemical properties of these analogues, several oligodeoxynucleotides were prepared from the phosphoramidite derivatives of **1** and **2**. Their intact incorporation into DNA was confirmed by electrospray mass spectrometry (ESI MS) and by proton NMR (see Supporting Information). For stacking studies, compounds **1** and **2** were studied in short self-complementary duplexes at a 5′ end dangling position as nearest neighbors to a C-G pair. For studies of pairing, the compounds were included into two nearest-neighbor contexts of a 12-bp duplex and were paired opposite each of the four natural bases separately.

Stacking studies revealed that both compounds, in presumed (but not confirmed) syn conformation at the ends of a duplex, stacked relatively strongly (see Table S1 in Supporting Information for data). Compound **2** added 12.1 °C in thermal stabilization to the melting transition temperature (T_m) of the core duplex for two substitutions, while the chlorofluoroindole base of **1** increased T_m by 17.1 °C and increased stability by −3.5 kcal/mol for two substitutions. For comparison, adenine (the strongest stacking of the natural nucleobases) stabilizes this same sequence by 9.9 °C (−2.0 kcal/mol).[17] The chlorofluoroindole base of **1** stacks as strongly as some of the most avid nucleobase analogues of recent studies, including pyrene and nitroindole.[17] Analogous stacking data for 8-oxo-A and 8-oxo-G are not yet reported.

Pairing studies of **1** and **2** were carried out near the center of 12-mer duplexes, with thermal denaturation experiments used to measure melting transition temperatures (T_m) and estimated free energies associated with helix stability. Data for one of the two contexts are given in Table 1, and examples of denaturation curves are given in Supporting Information. In general, both **1** and **2** were destabilizing as compared with a natural A-T base pair: pairs with compound **1** show a drop of ca. 14 °C in T_m, and pairs with compound **2**, by ca. 16 °C depending on the partner. This is much the same as other (anti-oriented) nonpolar isosteres;[16] for example, the dA analogue dZ also yields a 14 °C lowering of duplex T_m (see Table 1 and Supporting Information). By comparison, 8-oxopurines also display destabilization in duplex DNA relative to undamaged bases; for example, oxoguanine-A (Figure 2) and oxoinosine-A pairs have been shown to lower T_m by 6−7 °C in short duplexes (albeit in a different sequence context),[10e] probably due to the syn geometry. The added destabilization with the current isosteres, which has been attributed to desolvation costs, is essentially the same as reported for other nonpolar DNA base analogues.[18]

Base pairing selectivity in DNA (in the absence of enzymes) depends on complementary hydrogen bonding, solvation, and pair geometry. Because of their relatively low polarity, compounds **1** and **2** (and dZ) provide a test of the electrostatic influences on 8-oxopurine pairing selectivity. We measured selectivity by separately pairing the analogues in synthetic duplexes opposite each of the four natural bases; comparison of differences in thermal and thermodynamic stability reveals any preferences in this context. Our experiments (Tables 1 and S2) showed that, like other nonpolar base analogues, the oxopurine isosteres also exhibit low selectivity. However, there was in both cases measurable selectivity for one base. For example, the 8-oxo-dG (or 8-oxo-dI) analogue **1** showed a 2.4−

(15) Hamm, M. L.; Rajguru, S.; Downs, A. M.; Cholera, R. *J. Am. Chem. Soc.* **2005**, *127*, 12220−12221.
(16) (a) Guckian, K. M.; Morales, J. C.; Kool, E. T. *J. Org. Chem.* **1998**, *63*, 9652−9656. (b) Guckian, K. M.; Krugh, T. R.; Kool, E. T. *J. Am. Chem. Soc.* **2000**, *122*, 6841−6847.
(17) Guckian, K. M.; Schweitzer, B. A.; Ren, R. X.-F.; Sheils, C. J.; Tahmassebi, D. C.; Kool, E. T. *J. Am. Chem. Soc.* **2000**, *122*, 2213−2222.
(18) (a) Kool, E. T.; Morales, J. C.; Guckian, K. M. *Angew. Chem., Int. Ed.* **2000**, *39*, 990−1009. (b) Woods, K. K.; Lan, T.; McLaughlin, L. W.; Williams, L. D. *Nucleic Acids Res.* **2003**, *31*, 1536−1540.

Scheme 1 [a]

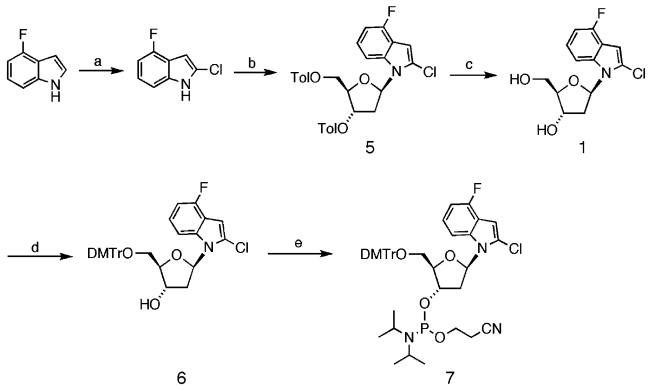

[a] Reagents and conditions: (a) (i) 1,1′-carbonyldiimidazole, THF, 70 °C (85%), (ii) $POCl_3$, 2,6-lutidine, 110 °C (46%); (b) NaH, CH_3CN, 0 °C, and Hoffer's chlorosugar, 0 °C (71%, N1/N3 > 20:1); (c) NaOMe, MeOH, THF (93%); (d) DMTrCl, pyridine (98%); (e) chlorodiisopropyl cyanoethylphosphoramidite, DIPEA, CH_2Cl_2 (59%).

Scheme 2 [a]

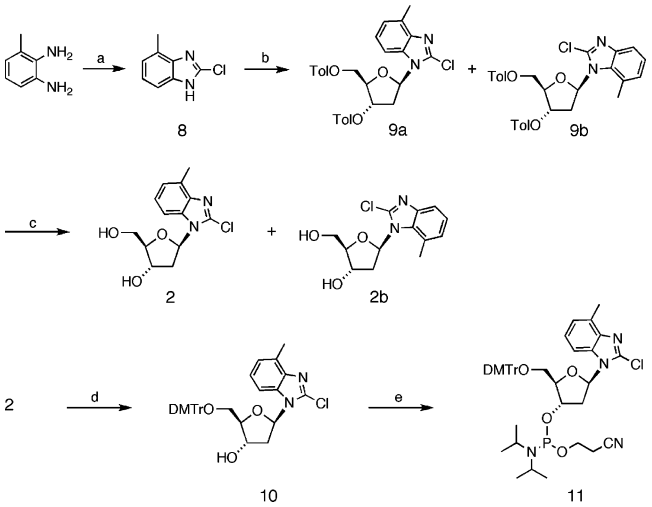

[a] Reagents and conditions: (a) (i) *n*BuLi, CO_2, THF, −78 °C, (ii) *t*BuLi, hexachloroethane, −78 °C (crude); (b) NaH, CH_3CN, 0 °C, and Hoffer's chlorosugar, 0 °C (84%, over two steps); (c) NaOMe, MeOH, THF (87%); (d) DMTrCl, pyridine (68%); (e) chlorodiisopropyl cyanoethylphosphoramidite, DIPEA, CH_2Cl_2 (68%).

3.9 °C (0.6−1.1 kcal/mol) preference for adenine as a partner rather than cytosine (although **1** is a guanine mimic) (Tables 1 and S2), presumably reflecting the thymine-like (rather than guanine-like) nature of the syn base. Significantly, an earlier study of natural 8-oxo-dI, the closest steric relative of analogue **1**, showed almost the same selectivity as we have observed for **1**, preferring to pair with A over C with a selectivity of 2.8 °C in T_m (0.5 kcal/mol in free energy).[10e] The oxo-dA analogue **2**, on the other hand, showed different selectivity in pairing: its preference was for G over T, with a T_m difference of 3.1−3.4 °C (0.4−0.6 kcal/mol). This selectivity is consistent with the C-like properties of the syn base, mimicking the mutagenicity of 8-oxo-A, although to our knowledge, no oligonucleotide pairing data for 8-oxo-A have yet been reported in the literature for comparison. Similar experiments with adenine analogue dZ, shown to be anti in solution and in DNA,[16] yielded little pairing preference for any one base (Tables 1 and S2).

Activity with DNA Pol I (Klenow Fragment). Of special interest is whether the altered shapes of these syn-oriented bases would affect their properties in DNA replication and how they would behave as compared with literature data for the natural oxidized purines. We therefore carried out steady-state kinetics studies of single-nucleotide insertions mediated by the Klenow fragment of DNA polymerase I (Kf exo$^-$). We tested compounds **1** and **2** (with comparison to dZ) in the DNA template strand as a probe of mutagenesis by oxidized purines in DNA, and we also studied nucleotides **3** and **4** as probes of misinsertion into new DNA caused by oxidative damage to the nucleotide pool. Full data are given in Tables 2 and 3; Figure 3 shows a graph of the insertion efficiencies (V_{max}/K_m) for these compounds paired opposite each of the four natural bases.

The experiments for the 8-oxo-dG analogue **1** in a template strand of DNA showed that the shape mimic directed preferential insertion of dATP (Table 2). As expected, the efficiency was

Table 1. Base-Pairing Properties in the Context of 12-Base-Pair DNA Duplex 5′ AAGAAXGAAAAG·5′CTTTTCYTTCTT[a,b]

base pair **X-Y**	T_m (°C)	$\Delta G°_{37}$ (kcal/mol)	$\Delta H°$ (kcal/mol)	$\Delta S°$ (kcal/mol)
Z-A	26.8	−6.1 ± 0.1	−67 ± 3	−196 ± 11
Z-G	27.3	−5.9 ± 0.1	−75 ± 3	−224 ± 9
Z-C	24.6	−5.4 ± 0.2	−71 ± 5	−211 ± 17
Z-T	25.0	−5.4 ± 0.1	−71 ± 4	−212 ± 14
2-A	24.9	−5.5 ± 0.1	−70 ± 3	−209 ± 10
2-G	27.6	−6.3 ± 0.1	−65 ± 2	−190 ± 7
2-C	24.9	−5.7 ± 0.1	−66 ± 2	−194 ± 7
2-T	24.5	−5.6 ± 0.1	−68 ± 3	−200 ± 6
1-A	29.8	−6.7 ± 0.1	−71 ± 2	−206 ± 5
1-G	26.4	−6.2 ± 0.1	−63 ± 2	−182 ± 6
1-C	25.9	−6.1 ± 0.1	−63 ± 2	−183 ± 7
1-T	26.2	−6.1 ± 0.1	−63 ± 2	−184 ± 7
T-A[c]	41.2	−9.4 ± 0.1	−84 ± 5	−241 ± 15
C-G[c]	43.0	−9.7 ± 0.1	−69 ± 6	−192 ± 18

[a] Conditions: 100 mM NaCl, 10 mM $MgCl_2$, 10 mM PIPES·Na (pH 7). T_m values are for 5.0 μM oligonucleotide. Averages of values from van't Hoff plots with five data points and curve fitting methods. [b] See Supporting Information for data on the same analogue pairs in a second context. [c] Data from ref 23.

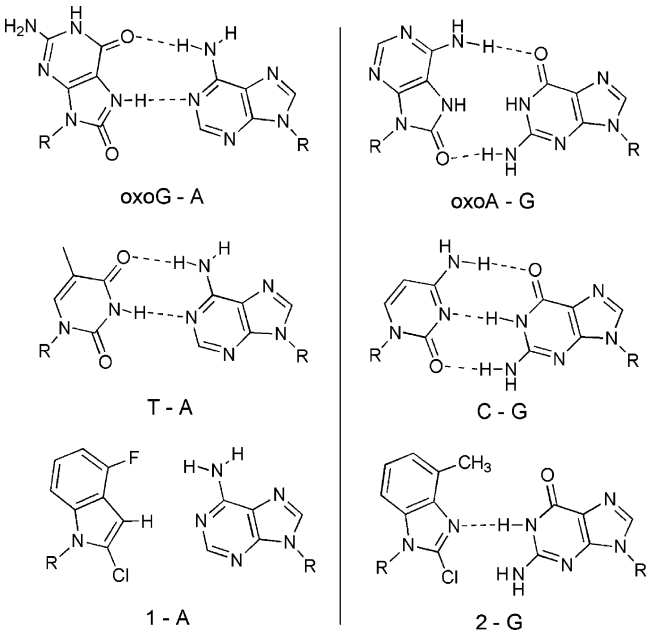

Figure 2. Mutagenic base-pairing structures involving *syn*-oxopurines, with comparison to natural T-A and C-G pairs. At the bottom are proposed analogous structures of the analogue pairs, illustrating their pairing and replication preferences. Note that for the *syn*-oxoA−G pair there is also a "wobble"-type structure possible (not shown). R = deoxyribose.

Table 2. Steady-State Kinetics Data for Insertion of Natural Nucleotides Opposite Modified Nucleoside Analogues (in the Template Strand) by the Klenow Fragment of DNA Pol I (exo$^-$)[a]

nucleoside triphosphate	template base (X)	V_{max}[b] (% min^{-1})	K_m (μM)	efficiency (V_{max}/K_m)	rel efficiency
dGTP	Z	0.032 (0.002)	64 (5)	5.0×10^2	8.6×10^{-3}
dATP	Z	0.7 (0.02)	39 (6)	1.7×10^4	3.0×10^{-1}
dCTP	Z	1.8 (0.2)	120 (30)	1.5×10^4	2.6×10^{-1}
dTTP	Z	5.8 (0.2)	100 (3)	5.8×10^4	1
dGTP	**2**	0.071 (0.001)	16 (12)	4.6×10^3	4.6×10^{-1}
dATP	**2**	0.31 (0.003)	32 (2)	9.9×10^3	1
dCTP	**2**	0.02 (0.0003)	34 (6)	5.7×10^2	5.8×10^{-2}
dTTP	**2**	0.044 (0.006)	63 (29)	7.0×10^2	7.0×10^{-2}
dGTP	**1**	0.019 (0.001)	36 (3)	5.2×10^2	2.2×10^{-2}
dATP	**1**	0.83 (0.008)	35 (2)	2.4×10^4	1
dCTP	**1**	0.018 (0.0001)	12 (2)	1.4×10^3	6.0×10^{-2}
dTTP	**1**	0.019 (0.001)	38 (5)	5.0×10^2	2.1×10^{-2}
dATP	dT	18 (2.3)	1.8 (1.6)	1.0×10^7	

[a] Conditions: 5 μM 23-mer/28-mer primer−template duplex, 0.05−0.2 units/μL Kf(exo$^-$), 50 mM Tris-HCl (pH 7.5), 10 mM $MgCl_2$, 1 mM dithiothreitol, 50 μg/mL BSA, and 100 μM dNTPs, incubated at 37 °C in a reaction volume of 10 μL. Standard deviations are given in parentheses. [b] Normalized for the lowest enzyme concentration used.

Table 3. Steady-State Kinetics Data for Insertion of Modified Nucleotide (dNTP) Analogues by the Klenow Fragment of DNA Pol I (exo$^-$)[a]

nucleoside triphosphate	template base (X)	V_{max}[b] (% min^{-1})	K_m (μM)	efficiency (V_{max}/K_m)	rel efficiency
dZTP	dG	0.067 (0.001)	56 (0.1)	1.2×10^3	1.6×10^{-1}
dZTP	dA	0.53 (0.001)	69 (1)	7.7×10^3	1
dZTP	dC	0.056 (0.001)	82 (0.4)	6.8×10^2	8.8×10^{-2}
dZTP	dT	0.18 (0.004)	56 (5)	3.2×10^3	4.1×10^{-1}
4	dG	0.2 (0.03)	33 (9)	5.9×10^3	1
4	dA	0.008 (0.0003)	53 (9)	1.5×10^2	2.6×10^{-2}
4	dC	0.004 (0.0001)	13 (2)	3.0×10^2	5.0×10^{-2}
4	dT	0.011 (0.001)	53 (12)	2.1×10^2	3.6×10^{-2}
3	dG	0.036 (0.001)	80 (12)	4.5×10^2	3.6×10^{-2}
3	dA	0.68 (0.08)	55 (9)	1.2×10^4	1
3	dC	0.006 (0.0001)	23 (3)	2.7×10^2	2.1×10^{-2}
3	dT	0.021 (0.001)	70 (14)	3.0×10^2	2.4×10^{-2}
dTTP	dA	17 (0.5)	2.3 (0.01)	7.4×10^6	

[a] Conditions: 5 μM 23-mer/28-mer primer−template duplex, 0.05−0.2 unit/μL Kf(exo$^-$), 50 mM Tris-HCl (pH 7.5), 10 mM $MgCl_2$, 1 mM dithiothreitol, 50 μg/mL BSA, and 100 μM dNTPs, incubated at 37 °C in a reaction volume of 10 μL. Standard deviations are given in parentheses. [b] Normalized for the lowest enzyme concentration used.

substantially lower than natural dATP insertion opposite T (by a factor of 10^3). However, this efficiency is higher than the relative efficiency reported for a template 8-oxo-G with this enzyme.[10b,e] Significantly, this preference mimics the mutational tendency of 8-oxo-G and 8-oxo-I to cause misinsertion of adenine[10,11] (although both A and C are inserted opposite the natural damaged bases).

Interestingly, chlorinated benzimidazole **2** in the DNA template yielded different results, directing preferential insertion of A and G as compared with C and T; thus **2** acts as a general pyrimidine analogue in this context (Table 2). This partly mimics the cellular mutagenesis by 8-oxo-A, which causes A → C transversions by mispairing with G.[12] The behavior of **2** is in direct contrast with dZ (the nonchlorinated species), which acted as an A analogue, directing insertion of dTTP with a small preference over C and A (Table 2).

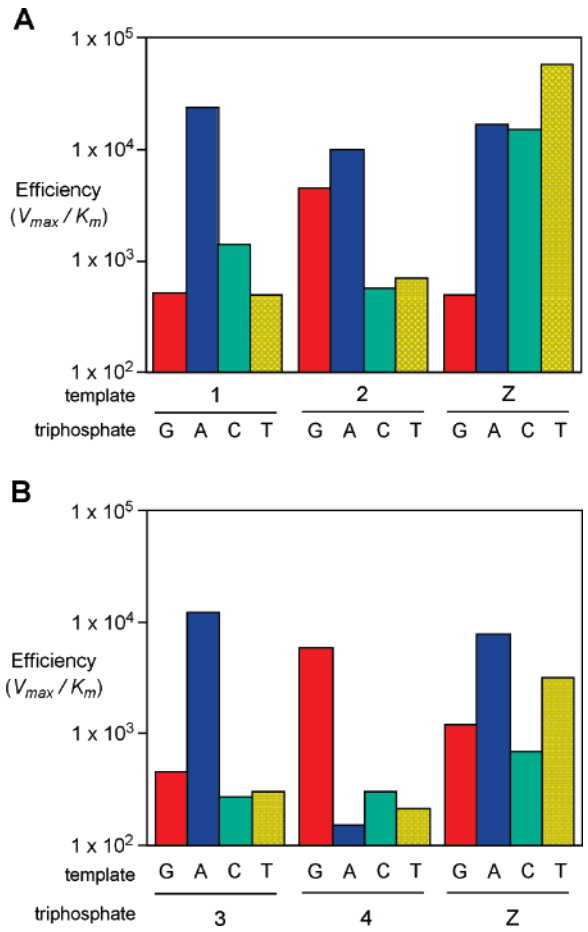

Figure 3. Mimicry by **1**−**4** of the mutagenic behavior of oxopurines in DNA replication. Shown are graphs of steady-state nucleotide insertion efficiency, mediated by the Kf(exo$^-$) polymerase. Efficiencies (V_{max}/K_m) are plotted on a log scale, with varied dNTP−template base pairings shown. (A) Data for oxopurine isosteres **1** and **2** in the template DNA, along with purine isostere dZ. (B) Data for oxopurine isostere nucleoside triphosphates (**3** and **4**) being inserted opposite natural bases in the template. See Tables 2 and 3 for numerical data.

Finally, nucleoside triphosphate compounds **3** and **4** were tested as analogues of damaged purines in the nucleotide pool. The dATP analogue *anti*-dZTP was studied for comparison. Results showed (Table 3, Figure 3) that compound **3** behaves very similarly to 8-oxo-dGTP in literature reports.[4] The analogue nucleotide was inserted selectively opposite adenine in the template (with a 40-fold preference over C or other bases); literature data indicate a similar 40-fold preference of 8-oxo-dGTP for a template adenine with this polymerase.[4b] The overall efficiency of **3** was only moderately (ca. 10-fold) lower than that reported for the natural damaged nucleotide. As for the 8-oxo-dATP analogue, **4** was preferentially incorporated opposite a template G, again consistent with its expected syn (C-like) shape. Although natural 8-oxo-dATP has yet to be studied kinetically, *syn*-**4** can be drawn in a pair opposite G in analogy to a *syn*-A-G pair (Figure 2) potentially formed by misinsertion of 8-oxo-dATP. The replication selectivity of nucleotide **4** was in marked contrast to that of the nonchlorinated dZTP, which was preferentially inserted opposite A and T (Table 3, Figure 3). Thus the results establish that the differences in shapes of these latter two compounds (likely arising from syn versus anti orientation) cause substantial effects in replication selectivity with this enzyme.

Discussion

Our experiments have shown that isosteric analogues of the 8-oxopurine nucleosides can effectively mimic several of the conformational, pairing, and mutagenic properties of the naturally damaged compounds. The structural mimicry by **1** and **2** of the syn preference was expected, since it was previously known that 8-chlorination of purines causes a change from anti to syn base orientation.[15] However, although both oxo and chloro substitution at this position yield a syn preference, it seems possible that chloro substitution may skew the anti−syn equilibrium further to the syn side. The longer bond and larger size of chloro is expected to cause a greater steric clash with the 5′ sugar substituent in anti orientation. This may also explain why the oxopurines show dual pairing and replication preferences, while the present chloroindole and chlorobenzimidazole compounds show a more singular preference for syn-like properties. For example, 8-oxo-G in a template directs polymerase incorporation of dCTP or dATP,[10] which could be explained by the base adopting either anti or syn orientation. It is widely recognized that *syn*-8-oxo-G resembles thymine in shape, size, and hydrogen-bonding potential, whereas the anti pairing edge of 8-oxo-G is indistinguishable from that of undamaged guanine. By comparison, analogue **1** directs incorporation of only dATP, which could be explained in part by a stronger preference for syn orientation. The syn pairing edge of **1** is quite close in size and shape to that of 8-oxo-G and also to thymine.

A similar argument can be made for the 8-oxo-A analogue **2**, which behaves in pairing and replication more as if it were cytosine than adenine. In syn orientation the pairing edge of **2** is close in shape and size to that of the pyrimidine base cytosine, whereas in anti orientation it would more closely resemble that of adenine. Indeed, in anti orientation **2** would have a pairing potential the same as the control compound Z, which behaves more as an adenine analogue. However, we observe that dZ and **2** behave quite differently in pairing and replication. This suggests strongly that the chloro group of **2** drives the conformation to syn in DNA and in the polymerase active site. This reflects the mutagenicity of 8-oxo-adenine, which is reported to cause A → C transversions.[11] *syn*-8-Oxo-adenine can be drawn in doubly hydrogen-bonded pairs with guanine (Figure 2), which might explain the origin of the transversion mutation. However, 8-oxo-A has a stronger preference for nonmutagenic behavior (directing preferential incorporation of T much more than G[11b]), while analogue **2** shows a more singular preference for mutagenic G incorporation behavior.

The mutagenic effects of oxidative damage to the purine nucleotide pool have been studied less than those of oxidized purines in existing DNA, in part because the concept is more recent. However, study of this phenomenon is increasing, and oxopurine nucleotides are under investigation as biomarkers of oxidative stress.[4,6] Our experiments show that shape analogues of 8-oxopurine nucleotides can be polymerase substrates and that they are selectively inserted opposite purines. This again suggests that these nucleotides occupy syn base conformations in the polymerase active site. It also suggests that these dNTP analogues might be generally useful as analogues of oxidized purines in the nucleotide pool, and specifically of the mutagenicity of this class of damaged compounds. Analogue **3** in particular behaves remarkably like its natural damaged congener, showing similar selectivity and efficiency. As a whole there is a need for greater study of oxopurine nucleotides; 8-oxo-dGTP has been studied kinetically with polymerases in only a few reports,[4] and we know of no reports of measurement of 8-oxo-dATP incorporation kinetics.

Our experiments with the Kf polymerase using analogues **1**−**4** suggest that much of the mutagenic properties of 8-oxo-G and 8-oxo-A in replication arises from steric (size and shape) effects of the bases in syn orientation. Our analogues in a DNA template effectively reproduce the mutagenic coding properties of the oxopurines, despite the fact that the analogue bases have little of the polar electrostatic properties of their natural analogues. Analogue **2** in syn orientation can form only one canonical hydrogen bond with G (Figure 2) and yet is more mutagenic than its natural congener. Analogue **1** in syn orientation can form no canonical hydrogen bonds with adenine but still directs preferential insertion of dATP. Note that we cannot rule out a small contribution from C−F−H−N and C−H−N interactions (see Figure 1), but we expect these to be quite weak in polar aqueous solution for a number of reasons.[19] First, the partial charges on F and on H attached to sp^2 carbon are quite small compared with canonical C═O and N−H; second, the polarization of the C−F group is much less than with C═O; and third, the high dielectric of water make such electrostatic effects weak in general. The observation of the mutagenic behavior in a system where electrostatic effects are greatly attenuated suggests that factors other than electrostatics may dominate this behavior.

More studies are needed to further explore the properties of analogues **1**−**4** in comparison to natural 8-oxopurine nucleosides and nucleotides. For example, it will be important in the future to study the analogues in replication by transient pre-steady-state kinetics methods, to obtain a clear picture of how the multiple steps of nucleotide insertion are affected by the altered electrostatics. In addition, it is recognized that different polymerases have different steric and hydrogen-bonding sensitivities,[20] and thus it will be of interest to study the analogues with enzymes from multiple genetic classes, including both repair and replicative enzymes. In addition, extension beyond damage lesions in DNA is an important activity that varies both with the specific form of damage and the polymerase; thus it will be worthwhile to study extension and editing kinetics as well. Moreover, beyond polymerases, it will be of significant interest to use these compounds as mechanistic probes of the various repair enzymes that recognize and process 8-oxopurines.[1,5,6]

In summary, we find that halogenated isosteres of polar purines act in a number of respects as effective biochemical mimics of 8-oxoguanine and 8-oxoadenine. Nucleosides incorporating them adopt syn geometry in solution (and likely so in DNA), as do the natural damaged nucleosides. The analogues pair in DNA with preferences that reflect the mutagenic syn pairing of the oxopurines and thus may be useful in probing enzymes that recognize and repair such damage in DNA. Third, in template DNAs during replication, they direct insertion of nucleotides that also reflect a mutagenic syn orientation, which can be useful in delineating the mechanisms of mutagenesis by

(19) Kool, E. T.; Sintim, H. O. *Chem. Commun.* **2006**, 3665−3675.
(20) (a) Ling, H.; Boudsocq, F.; Woodgate, R.; Yang, W. *Cell* **2001**, *107*, 91−102. (b) Johnson, S. J.; Beese, L. S. *Cell* **2004**, *116*, 803−816. (c) Kim, T. W.; Brieba, L. G.; Ellenberger, T.; Kool, E. T. *J. Biol. Chem.* **2006**, *281*, 2289−2295. (d) Mizukami, S.; Kim, T. W.; Helquist, S. A.; Kool, E. T. *Biochemistry* **2006**, *45*, 2772−2778.

oxidized purines. Finally, these isosteres can act as functional mimics of oxidative damage in the nucleotide pool and thus may be useful in studies of repair and mutagenesis from that source as well. The low polarity of these compounds will make them useful in probing the importance of electrostatic contributions in several biological damage response mechanisms.

Experimental Section

General Experimental Methods. Reagents and solvents were purchased from Aldrich and used without further purification. Thin-layer chromatography (TLC) was carried out on silica gel-60 F_{254} plates. Column chromatography was performed with silica gel, sizes 32−63. ^{1}H, ^{13}C, ^{19}F, and ^{31}P NMR spectra were recorded on Varian Mercury-400 or Inova-500 instruments as solutions in $CDCl_3$ and CD_3OD. Assignments of the anomeric stereochemistry and conformation about glycosyl bonds for compounds **1** and **2** were confirmed by 2D nuclear Overhauser effect (NOE) and correlation NMR spectroscopy (COSY) methods in DMSO-d_6 solution. High-resolution mass spectra were obtained at the University of California at Riverside MS Facility. HPLC purification was carried out on a Shimadzu HPLC instrument with reverse-phase C_{18} columns.

2-Chloro-1/3-[2′-deoxy-3′,5′-di-*O*-toluoyl-β-D-ribofuranosyl]-4-methyl-1*H*-benzimidazole (9a,b). To a solution of 2-chloro-4-methyl-1*H*-benzimidazole (**8**)[21] (200 mg, 1.2 mmol) in anhydrous CH_3CN (35 mL) was added NaH (33.4 mg, 1.32 mmol) at 0 °C. After the mixture was stirred for 30 min, Hoffer's chlorosugar (700 mg, 1.80 mmol)[22] was added in one portion at 0 °C. The reaction mixture was stirred at room temperature for 2 h and quenched by saturated $NaHCO_3$ solution and extracted with EtOAc. The organic layer was washed with water and brine, dried over Na_2SO_4, and concentrated under reduced pressure. The crude product was purified by column chromatography (silica gel, hexane/EtOAc 4:1) to yield **9a,b** (440 mg, 0.85 mmol, 71%) as a colorless foam containing N1 (**9a**) and N3 (**9b**) isomers (N1/N3 > 20:1). N1-isomer (**9a**, major peaks): ^{1}H NMR ($CDCl_3$, 400 MHz) δ 7.98−7.94 (m, 4H), 7.43 (d, 1H, J = 7.9 Hz), 7.28−7.23 (m, 4H), 7.00 (d, 1H, J = 7.9 Hz), 6.78 (t, 1H, J = 7.9 Hz), 6.50 (dd, 1H, J = 9.2, 5.9 Hz), 5.77−5.73 (m, 1H), 4.81 (dd, 1H, J = 12.2, 3.1 Hz), 4.74 (dd, 1H, ^{J} = 12.2, 3.8 Hz), 4.54−4.51 (m, 1H), 3.07 (ddd, 1H, J = 14.3, 9.2, 7.8 Hz), 2.57 (s, 3H), 2.53 (ddd, 1H, J = 14.3, 5.9, 2.1 Hz), 2.43 (s, 3H), 2.41(s, 3H). ^{13}C NMR ($CDCl_3$, 100 MHz) δ 166.36, 166.12, 144.68, 144.27, 141.42, 138.59, 132.57, 129.90, 129.87, 129.85, 129.41, 129.37, 126.83, 126.41, 123.76, 123.49, 109.37, 85.47, 81.83, 73.83, 63.77, 36.50, 21.85, 21.82, 16.58. HRMS (ESI+) *m/z* $[M + Na]^+$ calcd for $C_{29}H_{27}N_2O_5NaCl$ 541.1506, found 541.1509.

2-Chloro-1-[2′-deoxy-3′,5′-di-*O*-toluoyl-β-D-ribofuranosyl]-4-fluoroindole (5). *n*-Butyllithium (2.5 M hexane solution, 0.45 mL, 1.12 mmol) was added to a solution of 4-fluoroindole (150 mg, 1.11 mmol) in anhydrous tetrahydrofuran (THF) (3.0 mL) at −78 °C. The resulting suspension was kept at −78 °C for 30 min, and then CO_2 gas was bubbled through the mixture for 10 min. After being stirred for 10 min, the solvent was concentrated in vacuo at 0 °C. The residue was dissolved in anhydrous THF (3.0 mL), and then *t*-butyllithium (1.7 M pentane solution, 0.66 mL, 1.12 mmol) was added dropwise to this mixture at −78 °C. After the resulting yellow solution was held at −78 °C for 1 h, hexachloroethane (283 mg, 1.11 mmol) was added to the reaction mixture and it was stirred for 1 h at −78 °C. The reaction was quenched by water and saturated NH_4Cl solution and extracted with Et_2O. The organic layer was dried over $MgSO_4$ and concentrated in vacuo. This crude mixture was dissolved in anhydrous CH_3CN, and NaH (29.3 mg, 1.22 mmol) was added to this solution at 0 °C. After the mixture was stirred for 1 h, Hoffer's chlorosugar (561 mg, 1.44 mmol) was added in one portion at 0 °C. The reaction mixture was stirred at room temperature for 4 h and quenched by saturated $NaHCO_3$ solution and extracted with EtOAc. The organic layer was washed with water and brine, and it was dried over Na_2SO_4 and concentrated under reduced pressure. The crude mixture was purified by column chromatography (silica gel, hexane/EtOAc 4:1) to yield **5** (486 mg, 0.93 mmol, 84%) as a colorless foam: ^{1}H NMR [$CDCl_3$/tetramethylsilane (TMS), 400 MHz] δ 8.01−7.99 (m, 4H), 7.97 (d, 1H, J = 8.2 Hz), 7.43−7.27 (m, 4H), 6.77−6.68 (m, 2H), 6.57 (s, 1H), 6.53 (dd, 1H, J = 9.2, 5.9 Hz), 5.79−5.76 (m, 1H), 4.84 (dd, 1H, J = 12.2, 3.1 Hz), 4.76 (dd, 1H, J = 12.2, 3.8 Hz), 4.52−4.50 (m, 1H), 3.15−3.08 (m, 1H), 2.50−2.46 (m, 1H), 2.44 (s, 3H), 2.43 (s, 3H). ^{13}C NMR ($CDCl_3$, 100 MHz) δ 166.36, 166.14, 156.69, 154.22, 144.56, 144.21, 136.46, 136.36, 129.85, 129.37, 129.33, 126.91, 126.53, 124.62, 122.87, 122.80, 117.29, 117.06, 108.04, 106.24, 106.05, 98.38, 84.95, 81.27, 73.85, 63.83, 36.39, 21.82. ^{19}F NMR ($CDCl_3$, 376 MHz) δ −122.45 (dd, J = 9.2, 5.5 Hz). HRMS (ESI+) *m/z* $[M + Na]^+$ calcd for $C_{29}H_{25}NO_5FNaCl$ 544.1302, found 544.1311.

General Procedure for Removal of Toluoyl Groups. To a solution of the toluoyl compound (∼0.8 mmol) in anhydrous THF (3.0 mL) and anhydrous methanol (3 mL) was added $NaOCH_3$ (25% in CH_3OH, 0.5 equiv). The reaction mixture was stirred for 2 h at the room temperature, and then solid NH_4Cl was added to quench the reaction. This mixture was concentrated in vacuo to give the crude product. The mixture was purified by column chromatography (silica gel, CH_2Cl_2/CH_3OH 1:10). The structural identification of β anomer and conformation of glycosyl bond were measured by 2D NOE and COSY NMR methods in DMSO-d_6 solution.

2-Chloro-1-[2′-deoxy-β-D-ribofuranosyl]-4-methyl-1*H*-benzimidazole (2). The compound was isolated as a colorless foam: ^{1}H NMR (CD_3OD, 400 MHz) δ 7.67 (d, 1H, J = 7.9 Hz), 7.17 (t, 1H, J = 7.9 Hz), 7.08 (d, 1H, J = 7.9 Hz), 6.49 (dd, 1H, J = 8.5, 6.3 Hz), 4.56−4.53 (m, 1H), 3.95 (dt, 1H, J = 8.4, 3.9 Hz), 3.86−3.81 (m, 2H), 2.76 (ddd, 1H, J = 13.5, 8.5, 7.5 Hz), 2.53 (s, 3H), 2.25 (ddd, 1H, J = 13.5, 6.3, 2.9 Hz). ^{13}C NMR (CD_3OD, 100 MHz) δ 141.82, 140.12, 134.01, 129.86, 124.85, 124.72, 111.37, 88.52, 86.83, 71.92, 62.83, 39.60, 16.54. HRMS (ESI+) *m/z* $[M + H]^+$ calcd for $C_{13}H_{16}N_2O_3Cl$ 283.0849, found 283.0863. UV−visible (MeOH) ϵ = 6870 M^{-1} cm^{-1} at l = 260 nm.

2-Chloro-1-[2′-deoxy-β-D-ribofuranosyl]-4-fluoroindole (1). The compound was isolated as a colorless oil: ^{1}H NMR (DMSO-d_6, 400 MHz) δ 7.67 (d, 1H, J = 8.3 Hz), 7.15−7.10 (m, 1H), 6.90 (dd, 1H, J = 10.3, 8.0 Hz), 6.71 (s, 1H), 6.38 (t, 1H, J = 6.3 Hz), 5.38 (d, 1H, J = 4.3 Hz), 5.03 (t, 1H, J = 5.1 Hz), 4.39−4.38 (m, 1H), 3.81−3.80 (m, 1H), 3.68−3.63 (m, 2H), 2.60 (ddd, 1H, J = 13.3, 7.4, 6.3 Hz), 2.08 (ddd, 1H, J = 13.3, 6.3, 2.7 Hz). ^{13}C NMR (DMSO-d_6, 100 MHz) δ 153.46, 136.36, 136.28, 124.38, 122.75, 122.70, 115.95, 109.18, 105.67, 105.53, 97.17, 86.88, 84.36, 70.07, 61.28, 38.43. ^{19}F NMR (DMSO-d_6, 376 MHz) δ −122.92. HRMS (ESI−) *m/z* $[M + Cl]^-$ calcd for $C_{13}H_{13}NO_3FCl_2$ 320.0256, found 320.0267. UV−visible (MeOH) e = 9351 M^{-1} cm^{-1} at l = 260 nm.

General Procedure for Preparation of 5′-*O*-Tritylated Derivatives. To a solution of unprotected nucleoside (∼0.4 mmol) in pyridine (5.0 mL) was added 4,4′-dimethoxytrityl chloride (1.5 equiv) at room temperature. The mixture was diluted with EtOAc and successively washed with water and brine. The organic layer was dried over Na_2SO_4 and concentrated in vacuo, and then the crude product was purified by column chromatography (silica gel, CH_2Cl_2/CH_3OH containing 0.5% pyridine).

2-Chloro-1-[2′-deoxy-5′-*O*-(4,4′-dimethoxytrityl)-β-D-ribofuranosyl]-4-methyl-1*H*-benzimidazole (10). The compound was isolated as a colorless foam: ^{1}H NMR ($CDCl_3$/TMS, 400 MHz) δ 7.45 (d, 3H, J = 8.1 Hz), 7.37−7.33 (m, 4H), 7.29−7.21 (m, 3H), 7.01 (d, 1H, J = 7.4 Hz), 6.83−6.78 (m, 5H), 6.43 (dd, 1H, J = 8.1, 6.5 Hz), 4.73−4.71 (m, 1H), 4.05 (m, 1H), 3.78 (s, 6H), 3.54 (dd, 1H, J = 10.3, 4.2 Hz), 3.49 (dd, 1H, J = 10.3, 4.3 Hz), 2.80 (ddd, 1H, J = 13.8, 8.1, 5.9 Hz), 2.59 (s, 3H), 2.35 (br s, 1H), 2.28 (ddd, 1H, J = 13.8, 6.5, 3.1

(21) Ji, Q.; Li, J.; Huang, F.; Han, J.; Meng, J. *Synlett* **2005**, 1301−1305.
(22) Hoffer, M. *Chem. Ber.* **1960**, *93*, 2777−2781.
(23) Lee, A. H. F.; Kool, E. T. *J. Org. Chem.* **2005**, *70*, 132−140.

Hz). ^{13}C NMR ($CDCl_3$, 100 MHz) δ 158.66, 144.56, 141.31, 138.75, 135.68, 135.58, 132.64, 130.25, 129.54, 128.29, 128.02, 127.06, 123.59, 123.33, 113.30, 109.86, 86.85, 85.12, 85.08, 71.88, 63.15, 55.31, 38.94, 16.61. HRMS (ESI+) *m/z* $[M + Na]^+$ calcd for $C_{34}H_{33}N_2O_5NaCl$ 607.1975, found 607.1974.

2-Chloro-1-[2′-deoxy-5′-*O*-(4,4′-dimethoxytrityl)-β-D-ribofuranosyl]-4-fluoroindole (6). The compound was isolated as a colorless foam: ^{1}H NMR ($CDCl_3$/TMS, 400 MHz) δ 7.48−7.43 (m, 3H), 7.38−7.34 (m, 4H), 7.30−7.21 (m, 3H), 6.82 (dd, 4H, J = 8.8, 1.7 Hz), 6.76−6.71 (m, 2H), 6.55 (s, 1H), 6.49 (dd, 1H, J = 8.2, 6.7 Hz), 4.72−4.68 (m, 1H), 4.01−3.98 (m, 1H), 3.78 (s, 6H), 3.56−3.48 (m, 2H), 2.82 (ddd, 1H, J = 13.9, 8.2, 5.6 Hz), 2.21 (ddd, 1H, J = 13.9, 6.7, 3.2 Hz), 1.97 (d, 1H, J = 3.5 Hz). ^{13}C NMR ($CDCl_3$, 100 MHz) δ 158.66, 156.61, 154.16, 144.64, 136.41, 135.74, 135.65, 130.25, 128.30, 128.02, 127.05, 124.74, 122.65, 122.59, 117.17, 113.30, 108.50, 105.99, 105.80, 97.96, 94.51, 86.82, 84.54, 84.50, 72.09, 63.19, 55.31, 38.89. ^{19}F NMR ($CDCl_3$, 376 MHz) δ −122.87 (dd, J = 8.5, 7.3 Hz). HRMS (ESI+) *m/z* $[M + Na]^+$ calcd for $C_{34}H_{31}NO_5FNaCl$ 610.1772, found 610.1795.

General Procedure for Preparation of Phosphoramidite Derivatives. To a solution of the DMTr derivative (∼0.3 mmol) and *i*Pr_2NEt (3 equiv) in anhydrous CH_2Cl_2 was added *i*Pr_2NP(Cl)OC_2H_4CN (6 equiv) at 0 °C. After being stirred for 1 h at the same temperature, the reaction mixture was quenched with saturated $NaHCO_3$ solution and extracted with EtOAc. The organic layer was separated, dried over Na_2SO_4, and concentrated in vacuo. The crude compound was purified by column chromatography (silica gel, hexane/AcOEt) to give the purified material, which was precipitated from hexane at −78 °C. The hexane was removed by decantation and the solid material was dried in vacuum.

2-Chloro-1-[2′-deoxy-5′-*O*-(4,4′-dimethoxytrityl)-3′-*O*-(*N*,*N*-diisopropyl-β-cyanoethylphosphoramidyl)-β-D-ribofuranosyl]-4-methyl-1*H*-benzimidazole (11). The compound was isolated as a white powder: ^{1}H NMR ($CDCl_3$/TMS, 400 MHz) δ 7.58−7.52 (m, 1H), 7.48−7.41 (m, 2H), 7.37−7.15 (m, 7H), 6.99 (d, 1H, J = 7.5 Hz), 6.85−6.75 (m, 4H), 6.73−6.70 (m, 1H), 6.45−6.40 (m, 1H), 4.88−4.77 (m, 1H), 4.23−4.18 (m, 1H), 3.87−3.80 (m, 1H), 3.78 (s, 3H), 3.77 (s, 3H), 3.76−3.66 (m, 1H), 3.64−3.39 (m, 4H), 2.87−2.74 (m, 1H), 2.66−2.60 (m, 1H), 2.59 (s, 3H), 2.57−2.40 (m, 1.5H), 2.34 (ddd, 0.5H, J = 13.6, 5.3, 2.3 Hz), 1.25−1.12 (m, 9H), 1.06−1.04 (m, 2H), 0.88−0.83 (m, 1H). ^{13}C NMR ($CDCl_3$, 100 MHz) δ 158.62, 158.60, 144.51, 141.35, 138.65, 135.68, 135.65, 135.56, 135.51, 132.67, 130.37, 130.35, 130.32, 129.47, 129.44, 129.20, 128.45, 128.40, 127.94, 127.96, 127.15, 127.02, 126.98, 123.51, 123.27, 117.44, 113.21, 110.19, 86.71, 85.38, 85.32, 85.05, 84.75, 73.28, 73.10, 72.85, 72.66, 62.78, 62.59, 58.42, 58.26, 55.31, 55.28, 43.43, 43.35, 43.30, 43.22, 38.24, 24.67, 24.63, 24.55, 20.48, 20.41, 20.27, 20.19, 16.59. ^{31}P NMR ($CDCl_3$, 161 MHz) δ 149.39, 148.78. HRMS (ESI+) *m/z* $[M + Na]^+$ calcd for $C_{43}H_{50}N_4O_6NaPCl$ 807.3054, found 807.3041.

2-Chloro-1-[2′-deoxy-5′-*O*-(4,4′-dimethoxytrityl)-3′-*O*-(*N*,*N*-diisopropyl-β-cyanoethylphosphoramidyl)-β-D-ribofuranosyl]-4-fluoroindole (7). The compound was isolated as a white powder: ^{1}H NMR ($CDCl_3$/TMS, 400 MHz) δ 7.60−7.54 (m, 1H), 7.49−7.44 (m, 2H), 7.38−7.30 (m, 4H), 7.28−7.16 (m, 3H), 6.85−6.78 (m, 4H), 6.73−6.68 (m, 1H), 6.61−6.56 (m, 1H), 6.55 (s, 1H), 6.46−6.41 (m, 1H), 4.87−4.79 (m, 2H), 4.16 (t, 1H, J = 3.7 Hz), 3.78 (s, 3H), 3.77 (s, 3H), 3.63−3.50 (m, 4H), 3.47−3.43 (m, 1H), 2.89−2.80 (m, 1H), 2.60 (t, 1H, J = 6.6 Hz), 2.42 (t, 1H, J = 6.4 Hz), 2.37−2.29 (m, 0.5H), 2.28−2.24 (m, 0.5H), 1.25−1.12 (m, 9H), 1.06−1.04 (m, 2H), 0.88−0.83 (m, 1H). ^{13}C NMR ($CDCl_3$, 100 MHz) δ 158.65, 158.60, 158.59, 156.55, 154.11, 144.65, 144.61, 136.40, 135.77, 135.73, 135.66, 135.61, 135.56, 130.40, 130.37, 130.35, 129.20, 128.46, 128.43, 127.94, 126.98, 126.94, 126.94, 124.69, 124.66, 122.65, 122.57, 117.50, 117.46, 116.91, 113.25, 113.20, 108.97, 108.93, 105.94, 105.76, 98.05, 97.85, 94.50, 86.65, 84.90, 84.83, 84.62, 84.59, 84.36, 84.30, 73.27, 73.10, 72.84, 72.65, 62.79, 62.57, 60.47, 58.45, 58.26, 55.31, 55.28, 43.40, 43.32, 43.28, 43.20, 38.21, 24.71, 24.67, 24.62, 24.55, 22.71, 22.45, 22.37, 21.13, 20.46, 20.39, 20.25, 20.19, 14.27. ^{19}F NMR ($CDCl_3$, 376 MHz) δ −123.02 (dd, J = 9.8, 4.9 Hz), −123.08 (dd, J = 9.8, 4.9 Hz). ^{31}P NMR ($CDCl_3$, 161 MHz) δ 149.27, 148.60. HRMS (ESI+) *m/z* $[M + Na]^+$ calcd for $C_{43}H_{48}N_3O_6FNaPCl$ 810.2851, found 810.2875.

5′-Triphosphate Synthesis. The nucleoside (0.1 mmol) was stirred in trimethylphosphate (0.25 mL) with proton sponge (32 mg, 0.15 mmol) at 0 °C. $POCl_3$ (10 mL, 0.1 mmol) was added and the mixture was stirred for 2 h at 0 °C. A solution of tributylammonium pyrophosphate (240 mg) in anhydrous *N*,*N*-dimethylformamide (DMF) (1.0 mL) and *n*-tributylamine (0.1 mL) were added to the reaction mixture under vigorous stirring at 0 °C. After 5 min, 0.25 M aqueous triethylammonium bicarbonate (TEAB) buffer (10 mL) was poured into the solution. The aqueous layer was washed with dichloromethane (10 mL × 2) and concentrated under reduced pressure. The residue was purified by reverse-phase HPLC (Zorbox ODS 9.4 mm × 25 cm, SB-C18 column) with a linear gradient of CH_3CN/50 mM TEAA buffer (pH 7.5). The fractions containing triphosphate were collected and concentrated in vacuo. The residue of triethylammonium nucleoside triphosphate was dissolved in HPLC-grade methanol (0.2 mL) and precipitated by adding 0.6 M $NaClO_4$ solution in HPLC-grade acetone (1.2 mL). The precipitated sodium salt was collected by centrifugation, washed with acetone (1.0 mL × 4) and dried under vacuum.

2-Chloro-1-[2′-deoxy-β-D-ribofuranosyl]-4-methyl-1*H*-benzimidazole 5′-Triphosphate (4). ^{1}H NMR (D_2O, 400 MHz) δ 7.63 (d, 1H, J = 7.6 Hz), 7.29 (t, 1H, J = 7.6 Hz), 7.16 (d, 1H, J = 7.6 Hz), 6.55 (t, 1H, J = 7.4 Hz), 4.81−4.77 (m, 1H), 4.31−4.23 (m, 2H), 4.22−4.19 (m, 1H), 2.89−2.85 (m, 1H), 2.47 (s, 3H), 2.37−2.30 (m, 1H). ^{31}P NMR (D_2O, 161 MHz) δ −8.4, −13.4, −24.0. LRMS (ESI−) *m/z* $[M - H]^-$ calcd for $C_{13}H_{17}N_2O_{12}P_3Cl$ 520.0, found 520.6.

2-Chloro-1-[2′-deoxy-β-D-ribofuranosyl]-4-fluoroindole 5′-Triphosphate (3). ^{1}H NMR (D_2O, 400 MHz) δ 7.57−7.49 (m, 1H), 7.24−7.19 (m, 1H), 6.91−6.86 (m, 1H), 6.66 (s, 1H), 6.57 (dd, 1H, J = 8.4, 7.0 Hz), 4.81−4.77 (m, 1H), 4.29−4.22 (m, 2H), 4.15−4.14 (m, 1H), 2.96−2.89 (m, 1H), 2.28−2.22 (m, 1H). ^{19}F NMR (D_2O, 376 MHz) δ −123.5 (dd, J = 11.0, 4.9 Hz). ^{31}P NMR (D_2O, 161 MHz) δ −6.2, −11.0, −22.0. LRMS (ESI−) *m/z* $[M - H]^-$ calcd for $C_{13}H_{15}NO_{12}P_3ClF$ 524.6, found 524.3.

Oligodeoxyribonucleotide Synthesis. Oligonucleotides were synthesized by the standard DNA synthesis procedures (trityl-on mode) on an ABI 394 DNA/RNA synthesizer. Rapid-deprotecting chemistry was used [with PAC-A, Ac-C, and iPr-PAC-G phosphoramidites (Glen Research)]. Deprotection of synthesized oligonucleotides was done with 50 mM potassium carbonate in methanol (3 mL) at room temperature for 18 h. 5′-DMT oligonucleotides were purified by reverse-phase HPLC. The DMTr protecting group was cleaved in 10% aqueous acetic acid at room temperature for 30 min, the resulting DMTr-OH was removed by washing with ether, and the solvents were neutralized and concentrated under reduced pressure. Structures of the synthetic oligonucleotides were confirmed by ^{1}H NMR and matrix-assisted laser desorption ionization time-of-flight (MALDI-TOF) MS measurements (see Supporting Information for data).

Thermal Denaturation Experiments. Duplex DNA solutions were heated to 95 °C for 5 min and annealed by slow cooling (over 2 h to 5 °C). The melting studies were carried out in 1-cm path length quartz cells on a Varian Cary 100 Bio UV−vis spectrophotometer equipped with thermoprogrammer. The samples were warmed at a rate of 0.5 °C/min from 5 to 80 °C. Absorbance was monitored at 260 nm. The data were analyzed by the program MeltWin v. 3.0. Melting temperatures (T_m values) were determined by computer fit of the first derivative of absorbance with respect to 1/*T*. van't Hoff methods were used to calculate thermodynamic parameters.

Steady-State Kinetics Methods: 1. Steady-State Kinetics. Polymerase-catalyzed nucleotide single insertion reactions were carried out in 10 mL volumes in the reaction buffer [50 mM Tris-HCl (pH 7.5), 10 mM $MgCl_2$, 1 mM dithiothreitol, and 50 mg/mL BSA for Klenow (exo$^-$) DNA polymerase I (Amersham Bioscience)]. As polymerase

substrates we used 28-mer/23-mer template−primer duplexes having the sequence 5′-ACT GXT CTC CCT ATA GTG AGT CGT ATT A· 5′-TAA TAC GAC TCA CTA TAG GGA GA, where X is a variable nucleoside analogue or natural nucleoside. ^{32}P-End-labeled primer (final concentration ∼20 nM), template, and unlabeled primer were mixed in 2× reaction buffer and gave a final total concentration of template−primer of approximately 20 mM. The template−primer duplexes were annealed by heating to 90 °C and slow-cooled to 4 °C over 1 h. The commercial polymerase showed evidence of contaminating pyrophosphate in control reactions. By pretreating the polymerase enzyme with approximately 0.0002 unit of inorganic pyrophosphatase per unit of Kf for 10 min at 37 °C before addition of the template−primer duplex, interfering pyrophosphorolysis reactions were prevented. A 2× concentrated stock solution of duplex was mixed with 2× Kf(exo$^-$) polymerase, and the reaction was initiated by adding a 2× solution of the appropriate dNTP in the buffer (200 mM Tris-HCl, 20 mM $MgCl_2$, and 6 mM 2-mercaptoethanol, pH 7.5). Enzyme concentration and reaction time were adjusted in different dNTP reactions to give 1−20% incorporation in time periods ≤10 min. Additional data on nucleotide concentrations are given in Supporting Information. Reactions were quenched with loading buffer [80% formamide, TBE (89 mM Tris−borate and 2 mM EDTA), xylene cylanol, and bromophenol blue (pH 8)]. Extents of reaction were determined by running quenched reaction samples on a 20% denaturing polyacrylamide gel.

2. Kinetics Data Analysis. Radioactivity in primer and extended primer bands was quantified by use of a PhosphorImager (Molecular Dynamics) and the ImageQuant program. Relative velocity v was measured as the ratio of the extended product (I_{ext}) to remaining primer (I_{prim}) as follows $v = I_{ext}/I_{prim}t$, where t represents the reaction time, normalized for the lowest enzyme concentration used. The apparent K_m and V_{max} values were obtained from Hanes−Woolf plots.

Acknowledgment. This work was supported by the U.S. National Institutes of Health (GM072705). Y.T. acknowledges support from a JSPS postdoctoral fellowship.

Supporting Information Available: Spectra for characterization of nucleosides and nucleotides; spectra and characterization data for oligonucleotides; additional thermal denaturation data and curves; and detailed description of steady-state kinetics methods. This material is available free of charge via the Internet at http://pubs.acs.org.

JA071970Q